Laser and Particle Beams (2012), *30*, 489–495.

doi:10.1017/S0263034612000420

Numerical investigation for shape controlling of ultrathin electron layer

F. TAN, B. WU, B. ZHU, D. HAN, Z.-Q. ZHAO, W. HONG, L.-F. CAO, AND Y.-Q. GU
Research Center of Laser Fusion, China Academy of Engineering Physics, Mianyang, Sichuan, China

(RECEIVED 4 February 2012; ACCEPTED 1 June 2012)

Abstract

To control the shape of the ultra-thin electron layer produced by directly interaction of ultrahigh contrast laser with ultra-thin foil target, we investigated the spacial distribution and temporal evolution of electron layers produced from single and double foil targets through two-dimensional particle-in-cell simulations. Results show that electron layers produced from double foil targets can fly with unperturbed velocity for a much longer time than in the single foil case, which can be explained by the integrated contribution of charge separation field from both the two foils. Further studies show that through adjusting the foil expansion, electron layers with different shapes can be obtained. Detailed studies on the forming process of layers show that electron momentum distribution evolves rapidly along with the pump laser and then the vanishing of electron transverse momentum induced by the reflected laser results in the forming of layer shape. So different foil expansion corresponds to different moments that reflected laser interact with electron layer, when the electron transverse momentum distribution is different. After the reflected laser interact with electron layer, the resultant longitude momentum distribution will finally lead to various electron layer shapes.

Keywords: Laser-driven electron acceleration; Laser-plasma interactions; Nanofilm; Particle-in-cell method; Ultrathin electron layer

1. INTRODUCTION

X-ray source produced through Thomson scattering between high energy electrons and laser is a promising compact X-ray source with high energy, high brightness, and ultrashort duration of femtosecond time scale (Sprangle *et al.*, 1992; Sprangle & Esarey, 1992). It may be used to study atom and molecule motion on the femtosecond time scale, advanced biomedical imaging and lossless detection of high Z materials (Joshi & Corkum, 1995; Schoenlein *et al.*, 1996; Attwood, 1999). Such source has already been demonstrated through ultrashort lasers synchronized to an radio frequency electron gun (Leemans *et al.*, 1996; Ting *et al.*, 1996; Pogorelsky *et al.*, 2000; Chouffani *et al.*, 2002; Gibson *et al.*, 2004) or wakefield accelerated electrons (Schwoerer *et al.*, 2006). But due to the tiny cross-section of Thomson scattering and the low electron density, photon production of Thomson scattering source is too low for practical use.

To obtain higher photon yield, a possible method is using high density electron pulses accelerated from solid targets irradiated by ultraintense laser. Theoretical studies predict the possibility to produce ultrashort electron pulses from ultrathin foil targets (Kulagin *et al.*, 2007). Recently, the self-support diamond-like carbon foil (DLC) with thickness of nanometer scale (Liechtenstein *et al.*, 1997) has been applied into many ion, proton, electron acceleration, and high harmonic generation experiments. The results show many advantages upon thicker targets (Kiefer *et al.*, 2009; Hörlein *et al.*, 2011; Schnürer *et al.*, 2011; Steinke *et al.*, 2010). Such ultrathin foil targets requires ultrahigh contrast laser to prevent destroy from laser pre-pulse, so the recently developments on the few-cycle laser system with ultrahigh intensity, high contrast (Tavella *et al.*, 2007) make it possible to study the interaction between laser and ultrathin DLC foil targets.

For targets thin enough, the laser field $a_0 = eE_L/mc\omega_L$ can easily exceed charge separation field $E_{x0} = (n_e/n_c)k_L d$ on the targets, where e and m are electron charge and mass, c is velocity of light, E_L is laser electric field, $\omega_L = ck_L$ is the circular frequency of laser, n_e is electron density on the target, n_c is the critical density, and d is the initial foil thickness. Both fields are normalized. So all the electrons can be pushed out from the foil as a whole layer with high γ value (Kulagin *et al.*, 2007), where γ is the normalized electron energy. The

Address correspondence and reprint requests to: Y.-Q. Gu, Research Center of Laser Fusion, China Academy of Engineering Physics, Mianyang, Sichuan, China. E-mail: yqgu@caep.ac.cn

electron density in such layer is much higher than that in electron pulses accelerated from gas target or traditional electron accelerator. Experiments have been conducted by Kiefer *et al.* (2009), in which quasi-monochromatic electron pulses are obtained. If one introduces such electron layers into a Thomson scattering source as electron source, they can reflect probe laser and produce photons with energy blueshift up to $4\gamma^2$ due to Doppler shift. For the much higher electron density in the layers, such Thomson scattering X-ray source will work at the coherent Thomson scattering (CTS) regime (Wu & Meyer-ter-Vehn, 2009).

But there are two disadvantages for Thomson scattering source based on single foil model. First, due to the laser transverse electric field E_y, the accelerated electrons have large transverse momentum p_y, which will reduce the photon energy blueshift from $4\gamma^2$ to 2γ (Wu *et al.*, 2010). Second, due to charge separation effect and space charge effect, the electrons will be decelerated by the ions left behind and meanwhile expand. So the electron layers can only exist for a few tens of femtoseconds (Kulagin *et al.*, 2007), which increase the difficulty of synchronizing ultrashort lasers with electron pulses.

To overcome these disadvantages, researchers have proposed a modified model of double foil target (Meyer-ter-Vehn & Wu, 2009). In their model, after the pump laser pushes the electrons out of the first foil, it can be reflected by the second foil, and then interact with the electron layer for the second time, reducing electron transverse momentum p_y to nearly 0. After such interaction, the longitudinal component γ_x approximate to γ, leading to the maximum blueshift $4\gamma^2$ for the reflected photons.

Based on the double foil model, we compared the differences of electron layers from double and single foil targets and explored the corresponding origin. Then we investigated the way to control electron spacial distribution through adjusting the expansion between the two foils. Finally we studied the forming process of electron layers in detail and obtained the explanation for the forming of electron layers with different shapes.

2. SIMULATION PARAMETERS

Particle-in-cell (PIC) simulation has proven its validity in the studies of the interaction between ultrashort laser and ultrathin foil targets (Hörlein *et al.*, 2011; Schnürer *et al.*, 2011; Steinke *et al.*, 2010; Pae *et al.*, 2011; Wu *et al.*, 2010; Zhou weimin *et al.*, 2010). So we use PIC code VORPAL to study the electron acceleration process of ultrathin foil targets irradiated by ultrashort laser. In our work, the simulation box has a size of $20\lambda \times 20\lambda$ in the xy plane, and spacial resolution of 1000 cells/λ and 10 cells/λ in the x and y direction. The pump laser is linearly p-polarized along y direction and propagates from the left boundary of the simulation box to right, namely the $+x$ direction. This pulse has a profile $a_0 \sin^2(\pi t/T)$ with pulse duration $T = 4\lambda/c$, carrier envelop phase $\phi_0 = 0$, and wavelength $\lambda = 800$ nm. The transverse intensity profile is chosen as Gaussian $exp(-r^2/R^2)$, where $R = 5\lambda$ is the transverse half width at $1/e^2$ of maximum intensity. The normalized laser field a_0 is set to 3.5, corresponding to intensity of $I = 2.6 \times 10^{19}$ W/cm^2. Either single foil or double foil are used as target placed perpendicular to pump laser direction. The single foil is chosen with thickness $d_1 = 0.001\lambda$, density $n_{e1} = n_c$, and located at $x_1 = 5\lambda$. Double foil target is constructed with an thicker foil added to such single foil. The additional foil is chosen with thickness $d_2 = 0.03\lambda$, density $n_{e2} = 400n_c$, and located after the first foil. The spacing between the two foils d_0 is changed from 0.5λ to 4.0λ.

3. SIMULATION RESULTS AND ANALYSIS

First of all, the differences of finally obtained electron layers produced from single and double foil targets are shown as Figure 1. For single foil targets, Figure 1a and 1b show the maximum distance that the electron layers can reach. Afterward the layers will return and expand rapidly. At the chosen moment, electron energy in the layers is lower than 200 eV, and the central part of the layers are nearly static. Due to balance of space charge effect and magnetic force,

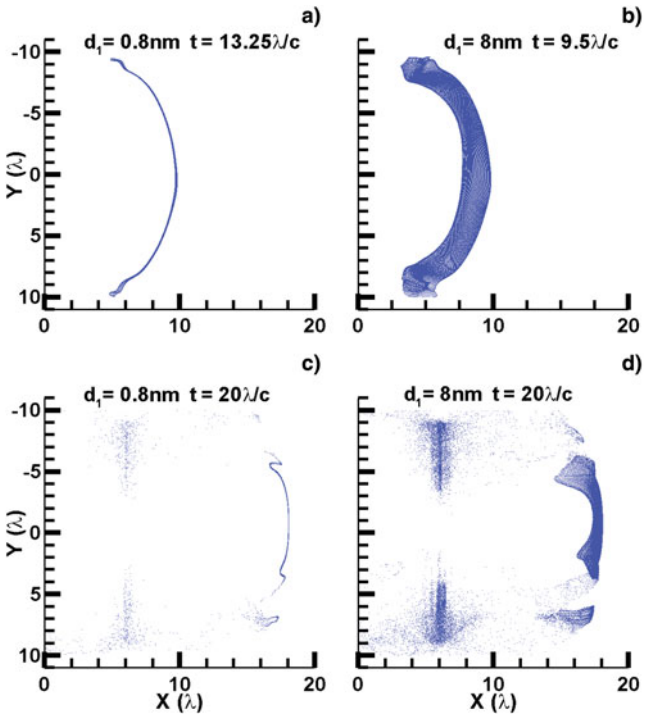

Fig. 1. (Color online) The spacial distribution of the accelerated electrons from single foil (**a**) and (**b**) and double foil (**c**) and (**d**). The upper row shows the farthest place that the electron layers can reach for the single foils with different thickness (a) $d_1 = 0.8$ nm (b) $d_1 = 8$ nm. The lower row shows the spacial distribution of steadily moving electron layers produced from double foil targets. The double foil targets are constructed from two foils that the first foil with different thickness (c) $d_1 = 0.8$ nm (d) $d_1 = 8$ nm and the thickness of the additional foil keeps $d_2 = 0.03\lambda = 24$ nm. The spacing between the two foils is $d_0 = \lambda = 800$ nm.

https://doi.org/10.1017/S0263034612000420 Published online by Cambridge University Press

the coulomb repulsion force F_s is (Chao & Tigner, 2006)

$$F_s = \frac{qE_s}{\gamma^2}, \tag{1}$$

where E_s is coulomb repulsion field in the pulse, direct proportional to foil thickness. So due to γ at denominator, electrons with small energy will suffer higher coulomb repulsion force and expand rapidly. Meanwhile, for thicker foil, coulomb repulsion force F_s is larger which lead to faster layer expansion, shown as Figure 1b.

But it is totally different for double foil case as Figure 1c and 1d. After produced from double foil targets, the electron layers can pass the second foil nearly unperturbed and move far from their original place, maintaining their shape for a much longer time ($\geq 20\lambda/c$). At the moment we chose, maximum electron energy in the layers is about 2 MeV, which reduces the space charge effect deeply. So it can be seen from Figure 1d, even when the foil thickness d_1 is as large as 8 nm, electron layer can still keep the layer-like shape and expand much slowly than in Figure 1b.

Electrons from the foil targets are mainly decelerated by the charge separation field, the differences of single and double foil targets show that the second foil may act like a shade from the charge separation field of the first foil, which cannot be achieved by a single plasma layer. Next we explored the origin of such differences. The electric fields near the foil and the spacial distribution of electron layers at different time for single and double foil targets are shown as Figure 2. For single foil target, the position of the field leading edge in Figure 2a corresponds to the own field of electron layer at $Y = -4 \times 10^{-6}$ in Figure 2(c). Laser electric field is subtracted from total field for clarity. Figure 2a shows that the charge separation field will continuously attract the electron layer, make it decelerate and finally return. But it is different for double foil target. In Figure 2b, the small peaks at $x = 4.67 \times 10^{-6}$ in thin line and $x = 4.9 \times 10^{-6}$ in thick line correspond to the own field of electron layer at $Y = 0$ in Figure 2d. At time $t = 7.4\lambda/c$, electron layer is moving with the laser. Then at time $t = 7.7\lambda/c$, after the electron layer passes the second foil, the field from the second foil overwhelms that from the first one, leading to repelling of the electrons. Then the integration field from the two foils decrease rapidly with farther distance. So at last the electron layers can move freely in space and reach much further place than those produced from single foil targets.

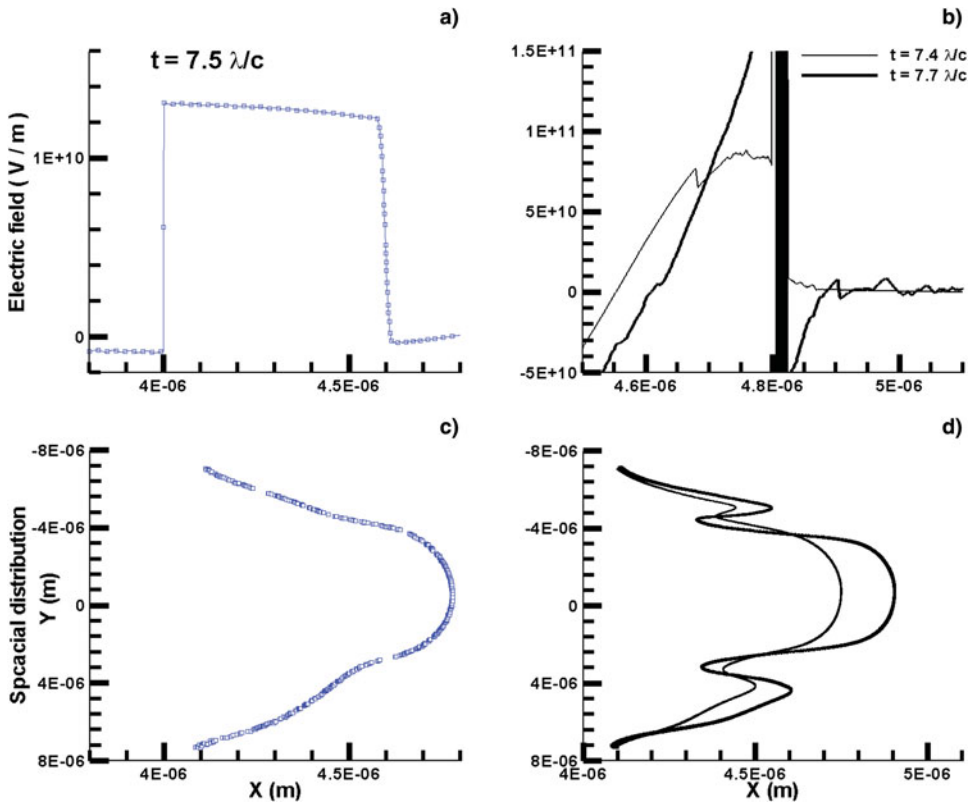

Fig. 2. (Color online) (upper row) The electric fields near the foil at different time and (lower row) the spacial distribution of electron layers at corresponding moment. The left column concerns single foil target at $t = 7.5\lambda/c$ and the right one concerns double foil target at $t = 7.4\lambda/c$ (thin line) and $t = 7.7\lambda/c$ (thick line). (**a**) The charge separation field between electron layer and single foil target at $Y = -4 \times 10^{-6}$. Laser electric field is subtracted from total field for clarity. (**b**) The electric field near the second foil at $Y = 0$. (**c**) The spacial distribution of electron layer produced from the single foil target. (**d**) The spacial distribution of electron layers produced from the double foil target. Laser and single/double foil parameters are the same as in Figure 1a and 1c.

https://doi.org/10.1017/S0263034612000420 Published online by Cambridge University Press

The studies above show the predominance of double foil targets. Then for further exploring the way to control electron layer shape, we studied in detail the forming process of electron layers produced from double foil targets. The following figures are all for double foil targets irradiated by ultraintense laser.

The finally obtained spacial distribution of electron layer for different foil expansion are shown as Figure 3. From Figure 3a we can see, when the two foils get close with each other, e.g., expansion $d_0 = 0.5\lambda$, the finally obtained electron layer looks like a concave mirror. According to Bulanov *et al.* (2003), high density concave electron layers can reflect counter-propagating laser convergently, leading to a promising way to obtain convergent X-ray and ultrahigh intense electric field at the focus. For a little larger foil expansion $d_0 = 1.0\lambda$ as in Figure 3b, nearly flat layer can be obtained, which may lead to reflected X-ray pulses with small divergence angle. If the foil expansion is equal to or higher than 2λ as in Figure 3c and 3d, electron layers will split into two or maybe more parts.

To explain the controlling of electron layer shape through adjusting foil expansion, next we investigated the temporal evolution of transverse and longitude momentum right before and after the interaction between reflected laser and electron layer happen, as Figures 4 and 5.

First, the forming process of concave layers as in Figure 3a is studied. When the second foil is close to the first one, expansion $d_0 = 0.5\lambda$, the temporal evolution of electron transverse and longitude momentum distribution is shown as Figure 4. From 4b to 4d, they show that the reflected laser interact with electron layer for the second time, eliminating the transverse momentum p_y in the regime $-3\lambda \le y \le 3\lambda$. Such elimination will lead to the increase of longitude momentum p_x, shown as the change from 4a to 4c. It notes that in

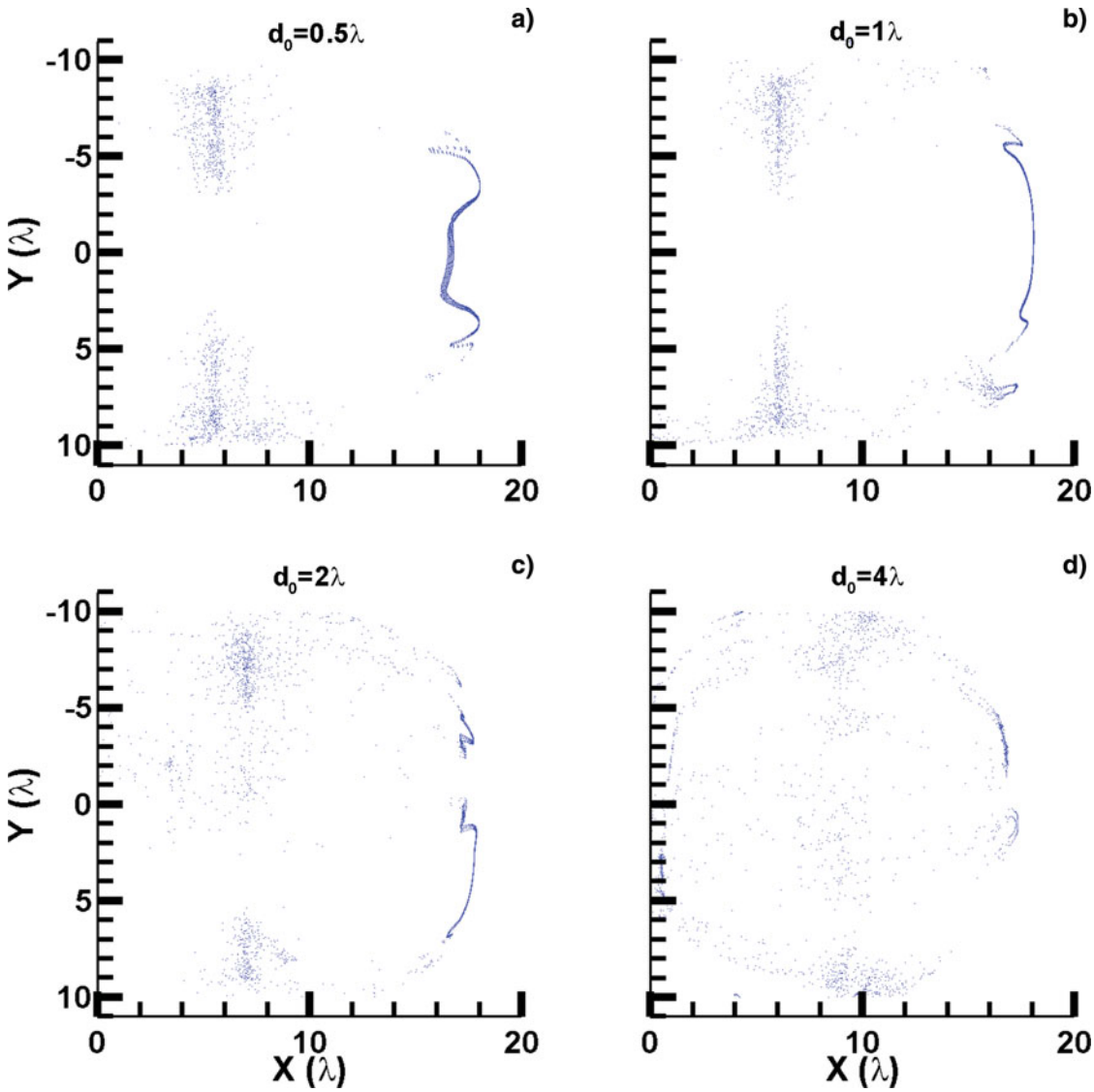

Fig. 3. (Color online) The electron spacial distributions finally obtained for the different spacing between the two foils in double foil targets. The spacing between the two foils are (**a**) $d_0 = 0.5\lambda$, (**b**) $d_0 = 1\lambda$, (**c**) $d_0 = 2\lambda$, and (**d**) $d_0 = 4\lambda$.

https://doi.org/10.1017/S0263034612000420 Published online by Cambridge University Press

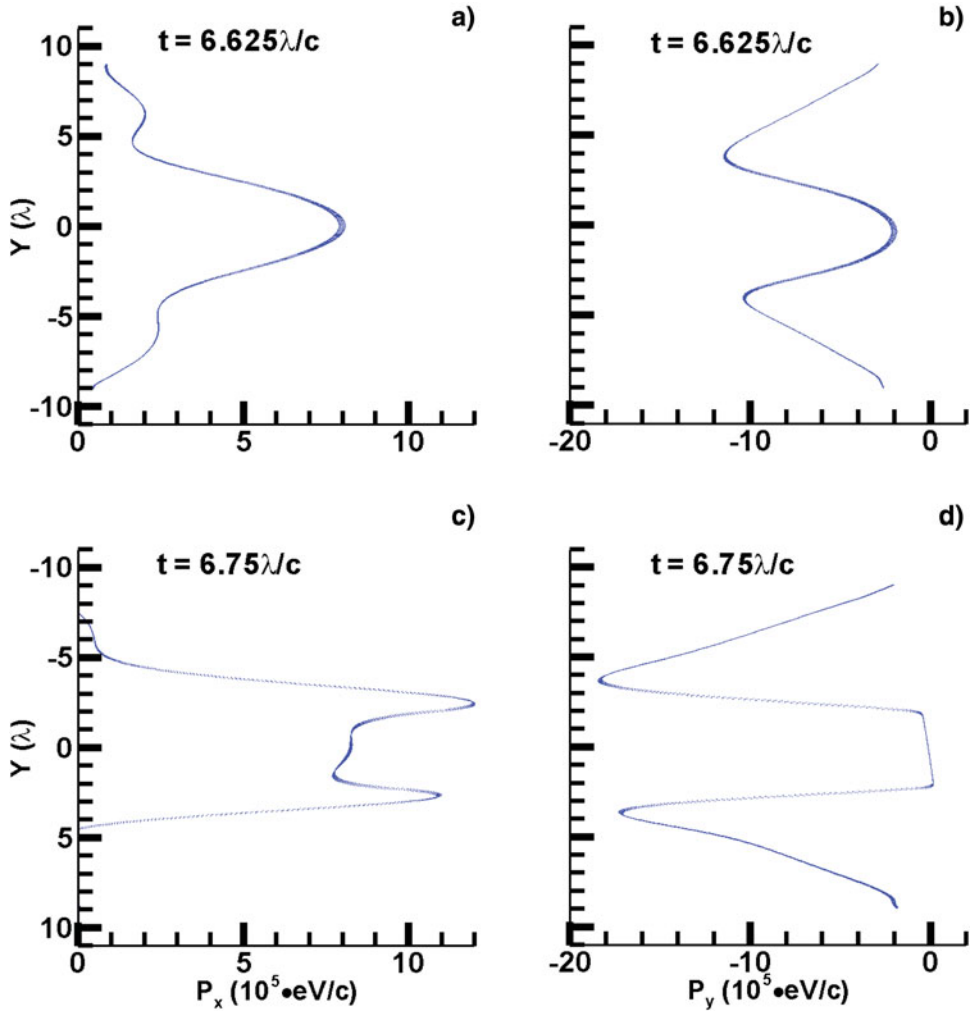

Fig. 4. (Color online) The electron longitude and transverse momentum distribution (**a**)(**c**)p_x and (**b**)(**d**)p_y along y-axis at the very momentum (**a**)(**b**) before and (**c**)(**d**) after the electron layer reach the second foil. Foil expansion is 0.5λ.

Figure 4b, at this moment $|p_y(x \approx 0)| \approx 0$, leading to nearly unchanged p_x after the elimination of p_y around this area. Meanwhile, $|p_y(x = \pm 3\lambda)| > |p_y(x \approx 0)|$, leading to two new peaks in longitude momentum distribution after the elimination of p_y as in Figure 4c. This double peak structure in longitude momentum distribution will finally lead to electron layers stably moving like a concave mirror. So the elimination of transverse momentum by the reflected pump laser can explain the forming of concave layers well.

Then, to explain the change of electron layer shape from concave to flat when d_0 is increased to 1.0λ, as in Figure 3b, the temporal evolvement of momentum distribution is also studied as in Figure 5. Different from Figure 4b, the central part of p_y in Figure 5b before interaction is nearly flat and the value is nearly 0. This different structure of p_y will lead to nearly unchanged p_x after p_y is vanished, shown in Figure 5 from 5a to 5c Finally, the p_x structure in Figure 5a will lead to nearly flat electron layers as in Figure 3b.

For double foil targets with foil expansion equal to or higher than 2λ, electron layer will evolve under the influence of laser field, leading to more complex momentum distribution of electrons in the layer. Then after the elimination of electron transverse momentum by the reflected laser, electron layers with more complex shape can be formed as in Figure 3c and 3d.

SUMMARY AND DISCUSSION

In summary, we compared the differences of the electron layers produced from single and double foil targets irradiated by ultrashort laser and found that the layers from double foil targets can reach much deeper place with higher energy. Further explorations reveal the origin of such differences. The electrons from single foil targets will be decelerated continually by strong charge separation field and form a so-called electron sheath behind targets. On the contrary, in double foil model, the total field from the two foils will decrease rapidly behind the second foil. The electron layers will be less influenced by charge separation field, leading to higher electron energy. So after the electron layers pass the second foil, they can move

https://doi.org/10.1017/S0263034612000420 Published online by Cambridge University Press

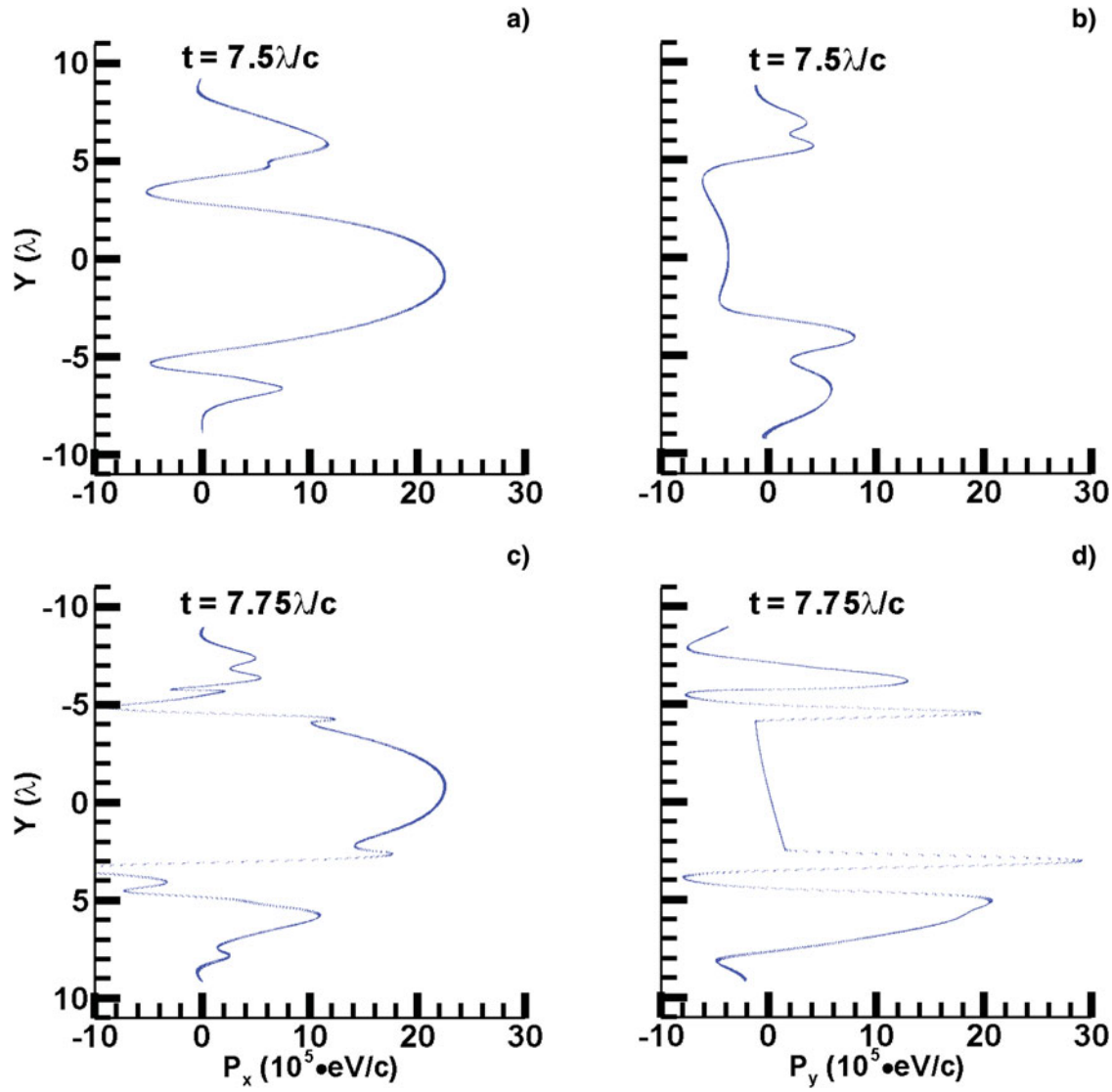

Fig. 5. (Color online) The same with Figure 4 but with different foil expansion $d_0 = 1.0\lambda$.

nearly unperturbed, keep the layer-like shape longer, and reach much deeper place. What's more, according to Wu's model, electrons' transverse momentum will be eliminated by the laser reflected by the second foil (Wu *et al.*, 2010). Obviously the resulting electrons with higher longitude momentum can also be less influenced by the charge separation field.

For target normal sheath acceleration, the electron sheath from single foil target will benefit the ion acceleration. But when apply the electron layers from single foil targets into Thomson scattering X-ray source as electron source, the energy of X-rays will be deeply reduced and the difficulty of synchronizing ultrashort lasers to electron pulses will increase. Compared with these disadvantages, the electron layers produced from double foil targets have large longitude momentum and longer flight, leading to X-ray sources with higher energy and easer synchronization. So the double foil targets irradiated by ultrashort laser are better electron source for Thomson scattering X-ray source.

Next, for the X-ray pulse shape depends on the shape of the electron source, it's necessary to study the way to control the shape of electron pulses in double foil model. In our method, through adjusting the expansion between the two foils, electron layers with different spacial distribution can be obtained. Further exploration on the mechanism shows that the elimination of electron transverse momentum p_y and the corresponding increasing of longitude momentum induced by the reflected laser respond for the forming of electron layer shape. It notes that due to the influence of laser field, electron momentum distribution varies rapidly. For different foil expansion, reflected laser interacts with electron layer at different time, when the instant momentum distributions are totally different. So the various momentum distributions will lead to electron layers with different spacial distributions.

With structure controlled electron layers as electron source, Thomson scattering X-ray source has the potentiality

https://doi.org/10.1017/S0263034612000420 Published online by Cambridge University Press

of producing X-ray pulses with controlled shapes, especially for hard X-ray pulses which are hard to converge. Our next work is further exploration on the electron layer shape control and the reflectivity of electron layers with various spacial distributions.

ACKNOWLEDGMENT

This work was supported by National Natural Science Foundation of China (Grant NO. 10902101 and 10774088).

REFERENCES

Attwood, D. (1999). *Soft X-rays and Extreme Ultraviolet Radiation: Principles and Applications*. Cambridge: Cambridge University Press.

Bulanov, S.V., Esirkepov, T. & Tajima, T. (2003). Light intensification towards the Schwinger limit. *Phys. Rev. Lett*. **91**, 085001.

Chao, A.W. & Tigner, M. (2006). *Handbook of Accelerator Physics and Engineering*. Singapore: World Scientific.

Chouffani, K., Wells, D., Harmon, F., Jones, J. & Lancaster, G. (2002). Laser-Compton scattering from a 20 MeV electron beam. *Nucl. Instrum. Methods Phys. Res. A*, **495**, 95–106.

Gibson, D.J., Anderson, S.G., Barty, C.P.J., Betts, S.M., Booth, R., Brown, W.J., Crane, J.K., Cross, R.R., Fittinghoff, D.N., Hartemann, F.V., Kuba, J., Sage, G.P.L., Slaughter, D.R., Tremaine, A.M., Wootton, A.J., Hartouni, E.P., Springer, P.T. & Rosenzweig, J.B. (2004). PLEIADES: A picosecond Compton scattering x-ray source for advanced backlighting and time-resolved material studies. *Phys. Plasmas* **11**, 2857–2864.

Hörlein, R., Steinke, S., Henig, A., Rykovanov, S.G., Schnürer, M., Sokollik, T., Kiefer, D., Jung, D., Yan, X.Q., Tajima, T., Schreiber, J., Hegelich, M., Nickles, P.V., Zepf, M., Tsakiris, G.D., Sandner, W. & Habs, D. (2011). Dynamics of nanometer-scale foil targets irradiated with relativistically intense laser pulses. *Laser Part. Beams* **29**, 383–388.

Joshi, C.J. & Corkum, P.B. (1995). Interaction of ultra-intense laser Light with matter. *Phys. Today* **48**, 36.

Kiefer, D., Henig, A., Jung, D., Gautier, D.C., Flippo, K.A., Gaillard, S.A., Letzring, S., Johnson, R.P., Shah, R.C., Shimada, T., Fernández, J.C., Liechtenstein, V.Kh., Schreiber, J., Hegelich, B.M. & Habs, D. (2009). First observation Of quasi-monoenergetic electron bunches driven out of ultra-thin Diamond-like carbon (DLC) foils. *Eur. Phys. J. D* **55**, 427–432.

Kulagin, V.V., Cherepenin, V.A., Hur, M.S. & Suk, H. (2007). Theoretical investigation of controlled generation of a dense attosecond relativistic electron bunch from the Interaction of an ultrashort laser pulse with a nanofilm. *Phys. Rev. Lett*. **99**, 124801.

Leemans, W.P., Schoenlein, R.W., Volfbeyn, P., Chin, A.H., Glover, T.E., Balling, P., Zolotorev, M., Kim, K.J., Chattopadhyay, S. & Shank, C.V. (1996). X-ray based subpicosecond electron bunch characterization using 90° Thomson scattering. *Phys. Rev. Lett*. **77**, 4182–4185.

Liechtenstein, V.K., Ivkova, T.M., Olshanski, E.D., Feigenbaum, I., Dinardo, R. & Döbeli, M. (1997). Preparation and evaluation of thin diamond-like carbon foils For heavy-ion tandem accelerators and time-of-flight spectrometers. *Nucl. Instrum. Meth. A* **397**, 140–145.

Meyer-ter-Vehn, J. & Wu, H.-C. (2009). Coherent Thomson backscattering from laser-driven relativistic ultra-thin Electron layers. *Eur. Phys. J. D* **55**, 433–441.

Pae, K.H., Choi, I.W. & Lee, J. (2011). Effect of target composition on proton acceleration by intense laser pulses in the radiation pressure acceleration regime. *Laser Part. Beams* **29**, 11–16.

Pogorelsky, I.V., Ben-Zvi, I., Hirose, T., Kashiwagi, S., Yakimenko, V., Kusche, K., Siddons, P., Skaritka, J., Kumita, T., Tsunemi, A., Omori, T., Urakawa, J., Washio, M., Yokoya, K., Okugi, T., Liu, Y., He, P. & Cline, D. (2000). Demonstration of 8×10^{18} photons/second peaked at 1.8Å in a relativistic Thomson scattering experiment. *Phys. Rev. ST Accel. Beams* **3**, 090702.

Schnürer, M., Andreev, A.A., Steinke, S., Sokollik, T., Paasch-Colberg, T., Henig, A., Jung, D., Kiefer, D., Hörlein, R., Schreiber, J., Tajima, T., Habs, D. & Sandner, W. (2011). Comparison of femtosecond laser-driven proton acceleration using nanometer and micrometer thick target foils. *Laser Part. Beams* **29**, 437–446.

Schoenlein, R.W., Leemans, W.P., Chin, A.H., Volfbeyn, P., Glover, T.E., Balling, D., Zolotorev, M., Kim, K.-J., Chattopadhyay, S. & Shank, C.V. (1996). Femtosecond X-ray pulses at 0.4 Å generated by 90° Thomson scattering. *Sci*. **274**, 236–238.

Schwoerer, H., Liesfeld, B., Schlenvoigt, H.-P., Amthor, K.-U. & Sauerbrey, R. (2006). Thomson-backscattered X rays from laser-accelerated electrons. *Phys. Rev. Lett*. **96**, 014802.

Sprangle, P., Ting, A., Esarey, E. & Fisher, A. (1992). Tunable, short pulse hard x-rays from a compact laser synchrotron Source. *J. Appl. Phys*. **72**, 5032–5038.

Sprangle, P. & Esarey, E. (1992). Interaction of ultrahigh laser fields with beams and plasmas. *Phys. Fluids B* **4**, 2241–2248.

Steinke, S., Henig, A., Schnürer, M., Sokollik, T., Nickles, P.V., Jung, D., Kiefer, D., Hörlein, R., Schreiber, J., Tajima, T., Yan, X.Q., Hegelich, M., Meyer-ter-Vehn, J., Sandner, W. & Habs, D. (2010). Efficient ion acceleration by collective laser-driven electron dynamics with ultra-thin foil targets. *Laser Part. Beams* **28**, 215–221.

Tavella, F., Nomura, Y., Veisz, L., Pervak, V., Marcinkevičius, A. & Krausz, F. (2007). Dispersion management for a sub-10-fs 10 TW optical parametric chirped-pulse Amplifier. *Opt. Lett*. **32**, 2227–2229.

Ting, A., Fischer, R., Fisher, A., Moore, C.I., Hafizi, B., Elton, R., Krushelnick, K., Burris, R., Jackel, S., Evans, K., Weaver, J.N., Sprangle, P., Esarey, E., Baine, M. & Ride, S. (1996). Demonstration experiment of a laser synchrotron source For tunable, monochromatic X-rays at 500 eV. *Nucl. Instrum. Methods Phys. Res., Sect. A* **375**, ABS68–ABS70.

Wu, H.-C. & Meyer-ter-Vehn, J. (2009). The reflectivity of Relativistic ultra-thin electron layers. *Eur. Phys. J. D* **55**, 443–449.

Wu, H.-C., Meyer-ter-Vehn, J., Fernández, J. & Hegelich, B.M. (2010). Uniform laser-driven relativistic electron layer for coherent thomson scattering. *Phys. Rev. Lett*. **104**, 234801.

Zhou, weimin, Gu, Yuqiu, Hong, Wei, Cao, Leifeng, Zhao, Zongqing, Ding, Yongkun, Zhang, Baohan, Cai, Hongbo & Kunioki, Mima. (2010). Enhancement of monoenergetic proton beams via cone substrate in high intensity laser, pulse-double layer target interactions, *Laser Part. Beams* **28**, 585–590.